

Liquid Core Photonic Quasi-Crystal Fiber Plasmonic Refractive Index Sensor for Wide Refractive Index Detection Range

Sanaz Shoar Ghaffari, Somaye Makouei

Faculty of Electrical and Computer Engineering, University of Tabriz, 51664, Tabriz, Iran

Corresponding author: Somaye Makouei (e-mail: makouei@tabrizu.ac.ir).

Abstract In this paper, a photonic quasicrystal fiber plasmonic refractive index sensor is numerically analyzed. The fiber core is infiltrated with six hypothetical liquids, the refractive indices of which vary from 1.44 to 1.49. The reason for filling the core with different refractive indexes of liquids is that a changeable refractive index of the core is an option to adjust the sensor performance at different intervals of analyte refractive index. Due to changes in the core refractive index, a large RI detection range from 1.38 to 1.53 is obtained and the sensor exhibits maximum spectral sensitivity of 10,000 nm/RIU. The properties of the refractive index sensor are calculated using the finite element method. The geometrical parameters of the sensor such as analyte height and gold thickness are also evaluated. The proposed sensor has a tunable capability which can be suitable for RI detection of biomedical liquid analytes in various ranges of refractive indices.

INDEX TERMS Finite element method, Photonic quasicrystal fiber, Refractive index sensor, Spectral sensitivity, Surface plasmon resonance, Tunable refractive index sensor.

I. INTRODUCTION

Surface Plasmon resonance waves are free electron oscillations at the interface of dielectric and a thin metal layer [1]. These evanescent waves are highly sensitive to refractive index changes of the medium near the surface of a metal layer. Surface Plasmon resonance (SPR) sensing has a great potential for various applications such as biosensing [2], bioimaging [3] medical diagnostics [4], biochemical and gas detection [5], [6]. Among the various methods of measuring the refractive index of different materials. SPR based fiber optic sensors have significant advantages over alternative methods such as electrochemical transistors [7], these advantages are remote sensing, long lasting, real time monitoring and ease of use. Also, the sensitivity of the surface plasmon waves to analyte changes is much higher than other methods. Conventional SPR sensors have the Otto and Kretschmann configuration based on prisms [8]. These sensors are bulky and are not suitable for remote sensing applications. In comparison, photonic crystal fiber-based sensors have the advantages of small size, flexible design, and remote sensing capability [9]. Consequently, in recent years, photonic crystal fiber-based surface Plasmon resonance (PCF-SPR) sensors have received significant research attention. There are a great number of papers have been published in this field [10], [11], [12], [13]. As a few examples, M. Liu *et al.* proposed a high sensitivity SPR biosensor with the analyte RI range of 1.4 to 1.43 [14]. Rifat

et al. reported a D-shaped PCF-SPR sensor in the visible to NIR wavelength range [15]. Most of the plasmonic photonic crystal-based structures are limited by the refractive index of the fiber material, which is usually fused silica. In this case, the detected refractive index (RI) range remains within the refractive index range of silica. Therefore, the sensor's ability to detect the RI range of analyte that is higher or lower than silica decreases. Monfared *et al.* proposed a D-shaped fiber optic plasmonic biosensor for high refractive index detection [16]. In the work, the photonic crystal fiber core is filled with the analyte whose refractive index is the target of detection to shift the RI detection range to higher indices. However, by placing the analyte in the core, the surface between metal and analyte separates and these sensors are not a suitable options for some applications such as biomolecular interaction detection. To the best of our knowledge, most of the refractive index sensors utilize structural changes for tunable sensing. For example, the output characteristics of the localized surface plasmon-based sensors can vary with size and shape of nanoparticles [17]. These structural changes are reported in ring resonators [18] and MDM waveguide-based sensors [19].

Once a sensor is made, characteristics are fixed. That is why, many plasmonic sensors are designed and each operating in a limited and specific RI range. The need for tunable sensors for sensing different refractive index ranges especially high

indices, is still a major challenge in the design of plasmonic sensors.

In this paper, a high sensitive rectangular channel photonic quasicrystal fiber-based (PQF) plasmonic refractive index sensor is proposed. The fiber core is filled with a reference liquid, which affects the regulation of sensor performance in detecting wide ranges of refractive indices. The numerical solution approach has been used for the fiber analysis. Although, there are some analytical methods for measuring the refractive index of materials, among which is the combination of semi-analytical model that is applied to predict the SPP generation in nanoledge plasmonic device and FDTD modelling for detection of refractive indices of common solvents [20], but these analytical models inevitably have to apply limiting assumptions that reduce the accuracy of the results. As another example, is analytical modeling of refractive index sensor based on Fabry-Perot Interferometer [21]. In the paper, the spectral response of microcavity is modelled by using the characteristic matrix method. In most of these analyzes, the authors had to use accurate numerical analysis or practical experiments to prove the accuracy of their analytical approach. In this paper, the FEM method is used to solve the Maxwell equations. Due to the complex structure of photonic crystal fibers and the periodic profile of the cladding refractive index, there is no clear boundary between the core and the cladding refractive index, so to obtain accurate modal analysis of the fiber, we have to solve equations by numerical methods such as FEM, which is possible through softwares such as Comsol Multiphysics. Thus, the FEM method is used for simulation where the number of complete mesh is 25196 domain elements and 1730 boundary elements. In the following, the geometry of the structure and the effect of RI variations in the core is investigated and spectral sensitivity with detection range is analyzed. Then, the influence of the analyte height on the profile of the sensor is studied. Finally, the effect of metal layer thickness has been reported.

II. THE GEOMETRY OF THE STRUCTURE

The cross section of the proposed refractive index sensor is shown in Fig. 1. The structure is six-fold PQF includes 4 layers of air holes that surround the core area. By examining different geometrical parameters and evaluating the desired result, the parameters are obtained: the diameter of the air hole is $d = 1 \mu\text{m}$, the core diameter, and the pitch of $d_c = 2.8 \mu\text{m}$, $\Lambda = 2 \mu\text{m}$ respectively. The radius of the entire sensor is $9 \mu\text{m}$. The channel height including air is $h = 6.1 \mu\text{m}$ and analyte height is $h_a = 0.45 \mu\text{m}$. A gold layer with a thickness of $t_{Au} = 0.05 \mu\text{m}$ is applied as plasmonic material.

The refractive index of fused silica is calculated by the sellmeier equation [22]:

$$n(\lambda) = \sqrt{1 + \frac{B_1^2}{\lambda^2 - C_1} + \frac{B_2^2}{\lambda^2 - C_2} + \frac{B_3^2}{\lambda^2 - C_3}} \quad (1)$$

where λ is an operating wavelength in micrometer. The constants are $B_1 = 0.69616300$, $B_2 = 0.407942600$, $B_3 = 0.897479400$, $C_1 = 0.00467914826$, $C_2 = 0.0135120631$ and $C_3 = 97.9340025$

A thin gold film is employed as a plasmonic material. The dielectric properties of the Au layer are described by the Drude - Lorentz model [23]:

$$\epsilon_{Au} = \epsilon_\infty - \frac{\omega_D^2}{\omega(\omega + j\gamma_D)} - \frac{\Delta\epsilon \cdot \Omega_L^2}{(\omega^2 - \Omega_L^2) + j\Gamma_L\omega} \quad (2)$$

where $\omega = 2\pi c/\lambda$, $\epsilon_\infty = 5.9673$, $\omega_D/2\pi = 2113.6 \text{ THz}$, $\gamma_D/2\pi = 15.92 \text{ THz}$, $\Delta\epsilon = 1.09$, $\Gamma_L/2\pi = 104.86 \text{ THz}$ and $\Omega_L/2\pi = 650.07 \text{ THz}$, respectively.

The air refractive index is set to 1 and the core liquid refractive index (n_c) varies from 1.44 to 1.49. A perfectly matched layer (PML) is used as a virtual radiation absorber. The performance of the proposed sensor is measured by the confinement loss (CL) spectrum of the fundamental mode by using (3) [24]:

$$L \left(\frac{\text{dB}}{\text{cm}} \right) = 8.686 \times \frac{2\pi}{\lambda(\mu\text{m})} \text{Im}(n_{eff}) \times 10^4 \quad (3)$$

where $\text{Im}(n_{eff})$ is the imaginary part of the effective refractive index of the mode.

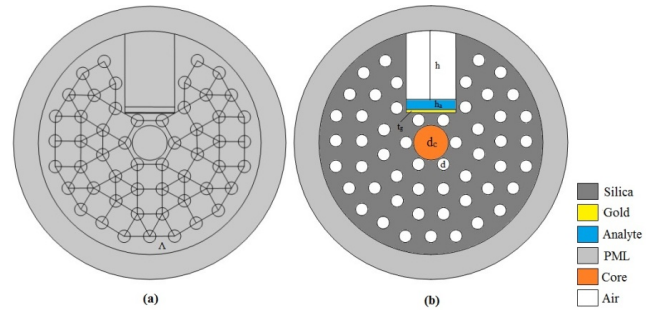


FIGURE 1. (a) Geometrical structure of the proposed PQF. (b) Sensor schematic diagram.

III. RESULTS AND DISCUSSION:

Surface Plasmon resonance occurs when the energy of the core mode becomes coupled to the plasmonic mode resulting in a peak in the confinement loss spectrum. This condition occurs when the real part of the effective refractive index of the core mode is equal to the real part of the effective refractive index of the plasmonic mode. Fig 2 shows the effective refractive indices of the core mode, plasmonic mode, and the confinement loss curve for the analyte refractive index of $n_a = 1.45$ and the core refractive index of $n_c = 1.46$. There is a peak in the confinement loss spectra at 967 nm .

The Plasmon resonance peak is sensitive to the surrounding dielectrics. In this work, the spectral sensitivity characteristics are investigated for the liquid core whose refractive index varies from 1.44 to 1.49. The core can be a

liquid solution whose refractive index is approximately constant in the operating wavelength range of the sensor [25]. Therefore, a tunable refractive index sensor is designed by changing the core material.

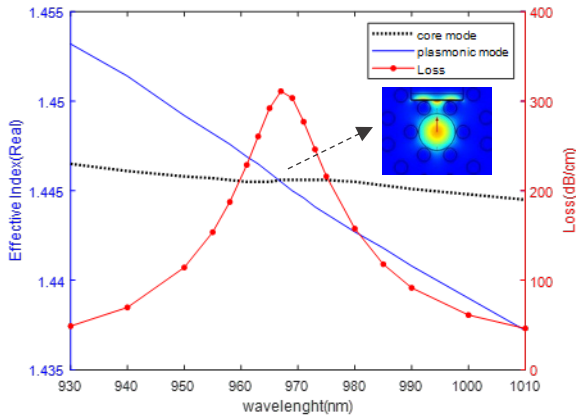


FIGURE 2. Distribution of the effective refractive index of the sensor and confinement loss diagram. ($d=2 \mu\text{m}$, $d_c=2.8 \mu\text{m}$, $h_a=0.45 \mu\text{m}$, $t_{Au}=0.05 \mu\text{m}$, $n_a=1.45$, $n_c=1.46$)

The spectral sensitivity of the sensor is expressed as [26]:

$$S_\lambda = \frac{\Delta\lambda_{peak}}{\Delta n_a} (nm/RIU) \quad (4)$$

where $\Delta\lambda_{peak}$ is the change of confinement loss peak wavelength and Δn_a is the change of analyte refractive index.

The confinement loss spectrum of different analytes for $n_c=1.47$ is shown in Fig. 3. As presented in Fig. 3, with increasing of n_a , CL peak of the spectrum moves towards the longer wavelength and almost constant spectral sensitivity of 3000 nm/RIU and detection range of 1.44 to 1.49 is achieved for the core refractive index of 1.47.

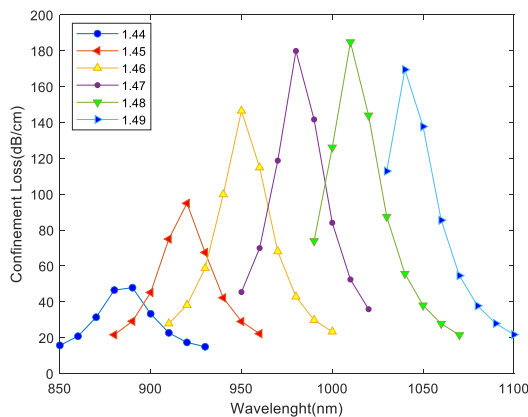


FIGURE 3. Fundamental mode confinement loss from $n_a=1.44$ to 1.49. ($d=2 \mu\text{m}$, $d_c=2.8 \mu\text{m}$, $h_a=0.45 \mu\text{m}$, $t_{Au}=0.05 \mu\text{m}$, $n_c=1.47$)

Sensitivity data of the sensor is reported in Table I, which shows sensor spectral output for core refractive index varies from 1.44 to 1.49. It is observed that for n_c intervals of 1.45 to

1.49, as the refractive index of the core increases, the detection range moves to higher refractive indices. Thus, at $n_c=1.49$, the sensor detection capability increases to measure the analyte RI of 1.53. The resonant wavelength range and spectral sensitivity are listed in the table as well.

TABLE I. Sensitivity data of PQF-SPR based Sensor

Core RI (n_c)	RI detection range (n_a)	Resonant wavelength range (nm)	Minimum wavelength sensitivity (nm/RIU)	Maximum wavelength sensitivity (nm/RIU)
1.44	1.43-1.46	980-1130	4000	6000
1.45	1.38-1.47	750-1090	1000	10000
1.46	1.40-1.47	750-1030	2000	9000
1.47	1.44-1.49	890-1040	3000	3000
1.48	1.44-1.51	850-1070	3000	4000
1.49	1.46-1.53	870-1110	3000	4000

The highest sensitivity of 10,000 nm/RIU is obtained for n_c of 1.45, the RI detection range being also wide in this case.

The channel intended for filling the analyte is a rectangular area, 4 micrometers wide. In order to investigate the effect of sample size, different heights of the analyte were analyzed. to evaluate the effect of analyte height on sensor performance, the spectral characteristics of the sensor have been investigated in different analyte heights of 0.35, 0.4, 0.45, 0.5, and 0.55 μm with $n_c=1.48$, and $n_a=1.48$. According to the results, the resonance wavelength depends on the height of the analyte and shifts with changes in height. Consequently, for proper separation of sample refractive index and according to the highest sensitivity reported, the height of the analyte must be fixed at a constant value. Fig. 4 shows that by enhancing the analyte height, CL peak value increases and the resonant wavelength shifts towards higher wavelengths.

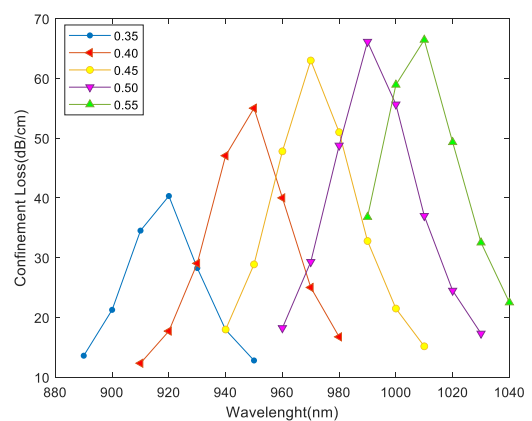


FIGURE 4. Confinement loss spectrum of the proposed sensor for analyte height variation of h_a from 0.35 to 0.55 μm . ($d=2 \mu\text{m}$, $d_c=2.8 \mu\text{m}$, $t_{Au}=0.05 \mu\text{m}$, $n_a=1.48$, $n_c=1.48$)

Metal film is an important geometric parameter in the optical properties of plasmonic sensors. Fig. 5 shows the dependence of optical confinement loss on the gold film thickness. As shown in the figure, by changing the thickness

of the gold layer, coupling between the core mode and plasmonic mode is changing. Confinement loss is investigated for three different thicknesses. It is observed that the coupling reduces with decreasing thickness of the gold layer.

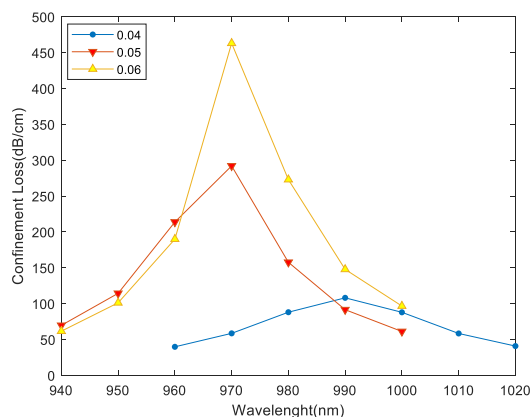


FIGURE 5. Dependence of confinement loss on the gold film thickness. ($d=2 \mu\text{m}$, $d_c=2.8 \mu\text{m}$, $h_a=0.45 \mu\text{m}$, $n_a=1.45$, $n_c=1.46$)

IV. CONCLUSION

A tunable and highly sensitive PQF-SPR refractive index sensor is proposed and numerically investigated using the FEM method. Variation in the core refractive index makes the sensor able to detect different ranges of analyte refractive indices. This feature is suitable for detecting analytes, especially with a high refractive index. A maximum spectral sensitivity of 10,000 nm/RIU and a large detection range from 1.38 to 1.53 are achieved. This proposed sensor has the potential to detect an extensive range of biological and chemical liquid analyte RIs by changing the refractive index of the liquid inside the core.

REFERENCES

- [1] E. Kretschmann, H. Raether, "Radiative decay of nonradiative surface plasmons excited by light," *Z. Naturforsch.* Vol. 12, pp. 2135-2136, 1968.
- [2] M. Skorobogaty and A. V. Kabashin, "Photonic crystal waveguide-based surface plasmon resonance biosensor," *Appl. Phys. Lett.*, Vol. 89, 143518, 2006.
- [3] S. Fang, et al., "Attomole microarray detection of MicroRNAs by nanoparticle-amplified SPR imaging measurements of surface polyadenylation reactions," *J. Am. Chem. Soc.*, Vol. 128, pp. 14044–14046, 2006.
- [4] A. Stephenson-Brown, et al., "Glucose selective surface plasmon resonance-based bisboronic acid sensor," *Analyst*, Vol. 138, pp. 7140–7145, 2013.
- [5] Z. Salamon, H. A. Macleod, and G. Tollin, "Surface Plasmon resonance spectroscopy as a tool for investigating the biochemical and biophysical properties of membrane protein systems. I: Theoretical principles," *Biochim. Biophys. Acta*, Vol. 1331, pp. 117–129, 1997
- [6] A. Nooke, et al., "On the application of gold based SPR sensors for the detection of hazardous gases," *Sensors and Actuators B: Chemical*, Vol. 149, pp. 194–198, 2020.
- [7] L. Zhang, et al., "Highly Selective and Sensitive Sensor Based on an Organic Electrochemical Transistor for the Detection of Ascorbic Acid," *Biosensors and Bioelectronic*, Vol. 17, 2018.
- [8] A. Otto, "Excitation of non-radiative surface plasma waves in silver by the method of frustrated total reflection," *Z. Phys.*, Vol. 216, pp. 398–410, 1968.
- [9] A. A. Rifat, et al., "Photonic crystal fiber-based plasmonic sensors," *Sens. Actuators B*, Vol. 243, pp. 311-325, 2017.
- [10] M. Tian, et al., "All-solid d-shaped photonic fiber sensor based on surface Plasmon resonance", *Opt. Commun.*, Vol. 285, pp. 1550–1554, 2012.
- [11] C. Liu et al., "Mid-infrared surface plasmon resonance sensor based on photonic crystal fibers," *Opt. Exp.*, Vol. 25, pp. 14227–14237, 2017.
- [12] D. J. J. Hu and H. P. Ho, "Recent advances in plasmonic photonic crystal fibers: Design, fabrication and applications," *Adv. Opt. Photon*, Vol. 9, 257–314, 2017.
- [13] A. Shafkat, "Analysis of a gold coated plasmonic sensor based on a duplex core photonic crystal fiber," *Sensing and Bio-Sensing Research*, Vol. 28, 100324, 2020.
- [14] M. Liu, X. Yang, and P. Shum, "High-sensitivity birefringent and single-layer coating photonic crystal fiber biosensor based on surface plasmon resonance," *Appl. Opt.*, Vol. 57, pp. 1883-1886, 2018.
- [15] A. A. Rifat, et al., "Highly sensitive D-shaped photonic crystal fiber-based plasmonic biosensor in visible to near-IR," *IEEE Sensors J.*, Vol. 17, pp. 2776–2783, 2017.
- [16] Y. E. Monfared, et al., "Quasi-D-Shaped Fiber Optic Plasmonic Biosensor for High-Index Analyte Detection," *IEEE Sensors*, Vol. 21, pp. 17-23, 2021.
- [17] S. Unser, et al., "Localized Surface Plasmon Resonance Biosensing: Current Challenges and Approaches," *Sensors*, Vol. 15, pp. 15684-15716, 2015
- [18] L. Hajshahvaladi, et al., "Design of a highly sensitive tunable plasmonic refractive index sensor based on a ring-shaped nano-resonator," *Optical and Quantum Electronics*, 2021.
- [19] X. Yi, et al., "Tunable fano resonance in MDM plasmonic waveguide with a T-shaped resonator coupled to ring resonator," *Materials Research Express*, pp. 1-15, 2018.
- [20] Z. Zeng, et al., "A semi-analytical decomposition analysis of surface plasmon generation and the optimal nanoledge plasmonic device," *J. The royal society of chemistry*, pp. 17196–17203, 2016.
- [21] E. V. Rodrig, et al., "Analytical Modelling of a Refractive Index Sensor Based on an Intrinsic Micro Fabry-Perot Interferometer," *Sensors*, Vol. 15, pp. 26128-26142, 2015.
- [22] S. Chakma, et al., "Gold-coated photonic crystal fiber biosensor based on surface plasmon resonance: design and analysis," *Sens. Bio-Sens. Res.*, Vol. 18, pp. 7–12, 2018.
- [23] M. S. Islam, et al., "A Hi- Bi ultrasensitive surface plasmon resonance fiber sensor," *IEEE Access*, Vol. 7, pp. 79084-79094, 2019.
- [24] X. Yang, et al., "Analysis of a graphene-based photonic crystal fiber sensor using birefringence and surface Plasmon resonance," *Plasmonics*, Vol. 12, pp. 489–496, 2017.
- [25] K. Moutzouris, et al., "Refractive, dispersive and thermo-optic properties of twelve organic solvents in the visible and near-infrared," *Appl. phys. B*, Vol. 116, pp. 617–622, 2014.
- [26] C. Liu, et al., "Theoretical assessment of a highly sensitive photonic crystal fiber based on surface Plasmon resonance sensor operating in the near-infrared wavelength," *J. Mod. Opt.*, Vol. 66, pp. 1–6, 2019.